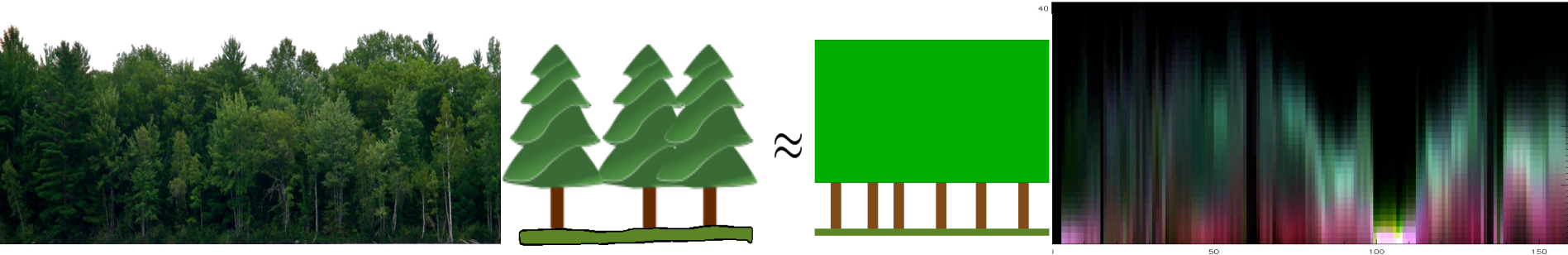


# Forest Structure Characterization using UAVSAR PolInSAR and Tomography



*Maxim Neumann*

*UAVSAR Team: Scott Hensley, Marco Lavallo, Razi Ahmed,  
Thierry Michel, Ron Muellerschoen, . . .*

*Jet Propulsion Laboratory, California Institute of Technology*

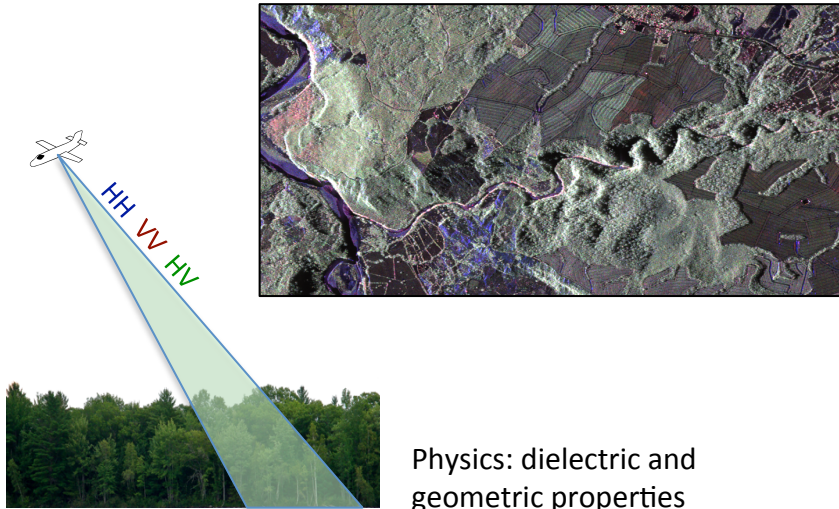
*UAVSAR Workshop  
03/27/2012 – Pasadena*



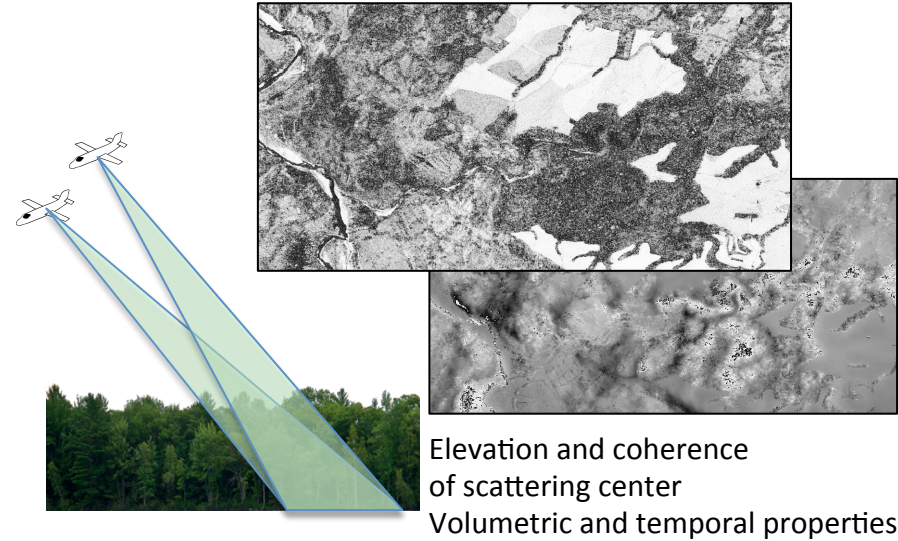


# Basic Principles

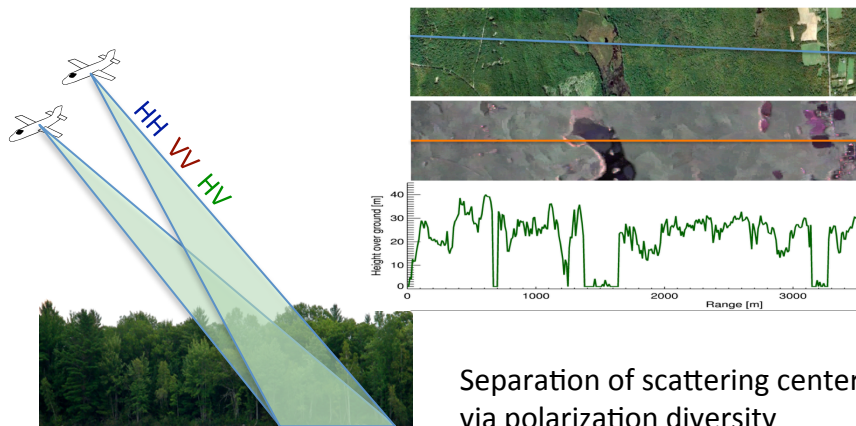
## Polarimetry



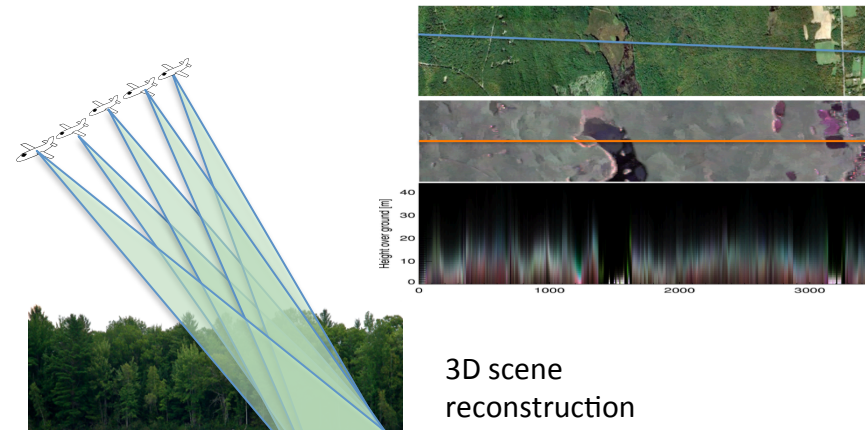
## Interferometry



## Polarimetric Interferometry



## Tomography

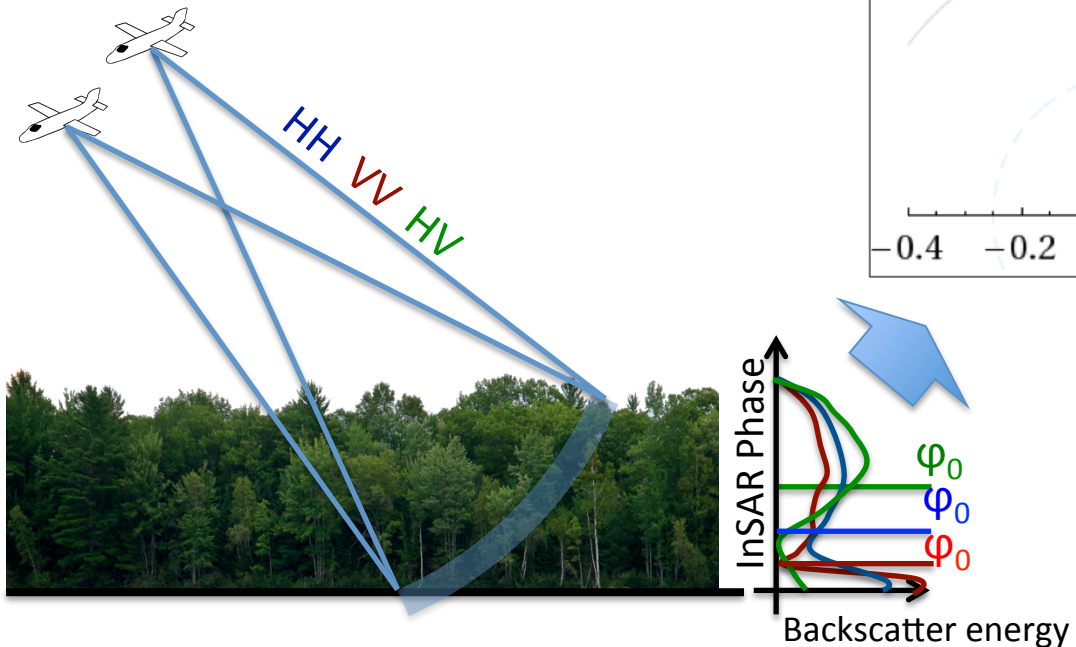




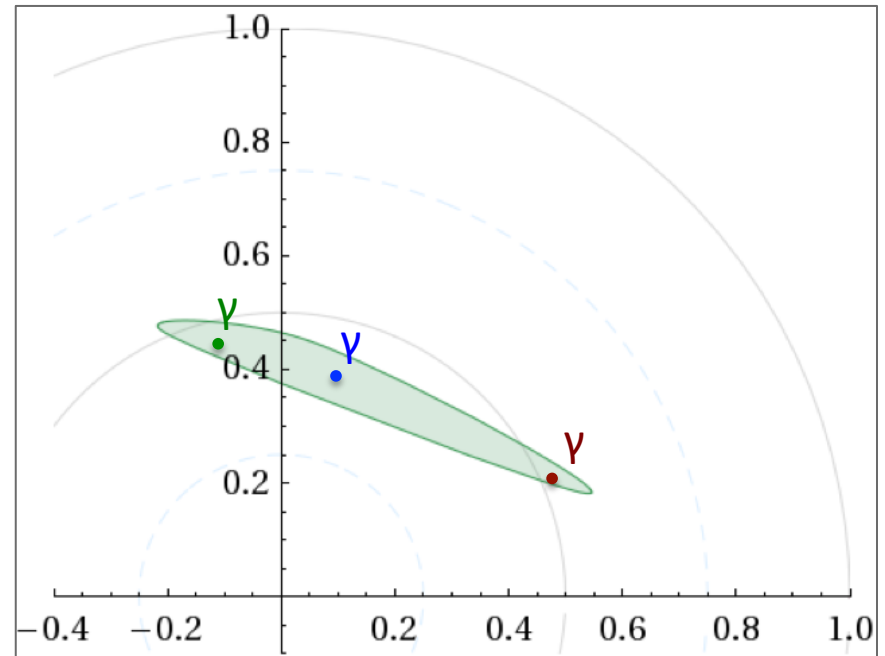
# PolInSAR Intro

## Polarimetric SAR Interferometry

$$\mathbf{T}_6 = \langle \mathbf{k} \mathbf{k}^\dagger \rangle = \begin{bmatrix} \mathbf{T}_{11} & \mathbf{\Omega}_{12} \\ \mathbf{\Omega}_{12}^\dagger & \mathbf{T}_{22} \end{bmatrix} \quad \mathbf{k}_i = \begin{bmatrix} HH_i \\ HV_i \\ VV_i \end{bmatrix}$$
$$\mathbf{k} = \begin{bmatrix} \mathbf{k}_1 \\ \mathbf{k}_2 \end{bmatrix}, \quad \gamma_{12}(\omega) = \frac{\omega^\dagger \mathbf{\Omega}_{12} \omega}{\sqrt{\omega^\dagger \mathbf{T}_{11} \omega \omega^\dagger \mathbf{T}_{22} \omega}}$$



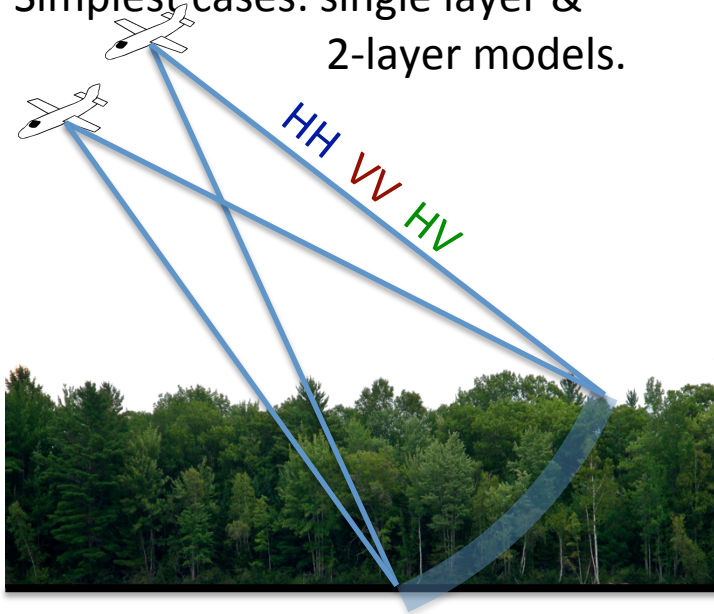
## Coherence Unitary Circle (CUC)



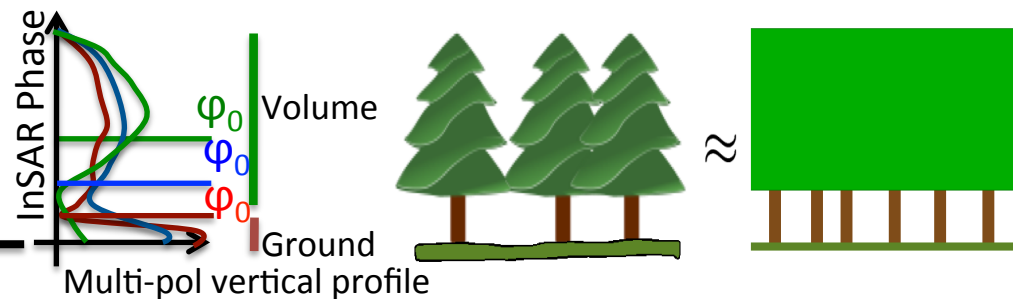
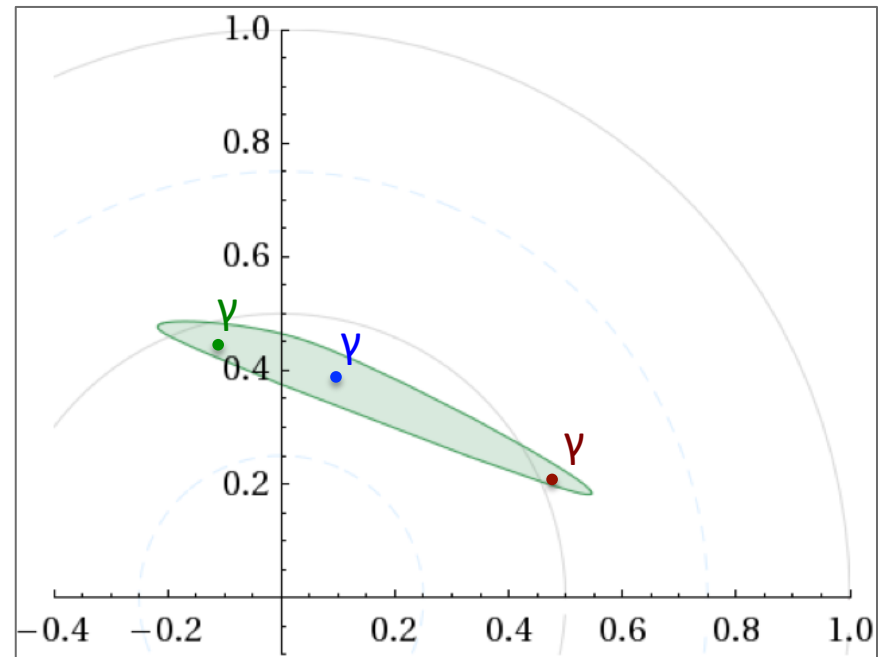


# PolInSAR Vegetation Model

- Multi-layer model:  $\mathbf{T} = \sum \mathbf{T}_i$
- Possible layer separation due to
  - vertical structure
  - temporal behavior
  - polarimetric characteristics
- Every medium can be characterized with  $i \rightarrow \infty \rightarrow$  unpractical!
- Simplest cases: single layer & 2-layer models.



Coherence Unitary Circle (CUC)





# 2-Layer PolInSAR Vegetation Model

## Assumptions:

- Ground and volume components not correlated
- Polarimetric stationarity
- No refraction effects and no differential extinction
- Volume and ground components homogeneous

## Model: Ground + Volume Layers

$$\mathbf{T}_6 = \begin{bmatrix} \mathbf{T} & \mathbf{\Omega} \\ \mathbf{\Omega}^\dagger & \mathbf{T} \end{bmatrix} \begin{cases} \mathbf{T} = \mathbf{T}_g + \mathbf{T}_v \\ \mathbf{\Omega} = \gamma_g \mathbf{T}_g + \gamma_v \mathbf{T}_v \end{cases}$$

$$= \mathbf{R}_g \otimes \mathbf{T}_g + \mathbf{R}_v \otimes \mathbf{T}_v \text{ with } \mathbf{R}_{g/v} = \begin{bmatrix} 1 & \gamma_{g/v} \\ \gamma_{g/v}^* & 1 \end{bmatrix}$$

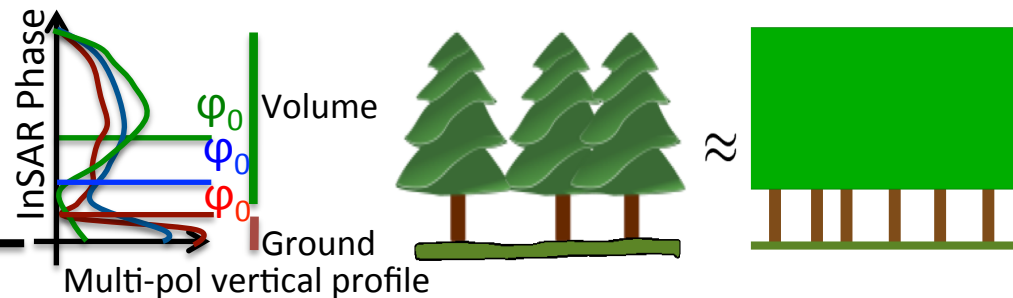
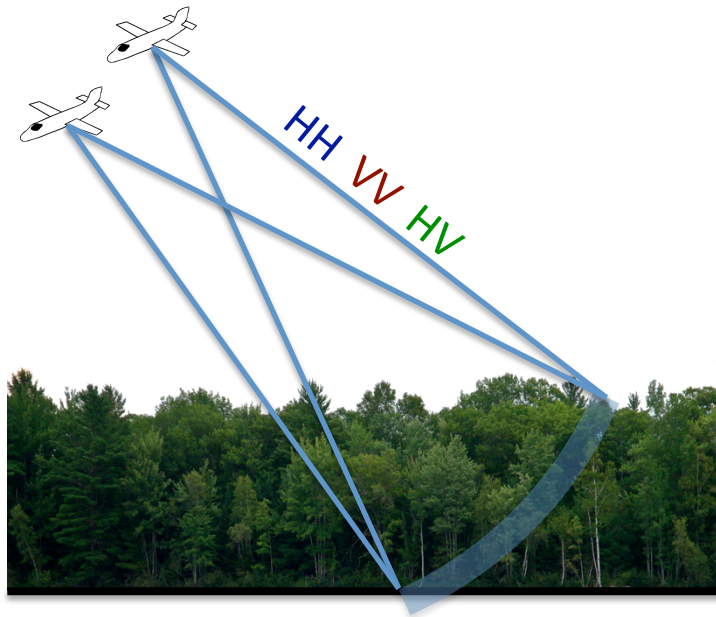
$\mathbf{T}_g/\mathbf{T}_v$ : ground and volume PolSAR cov matrices

$\gamma_g/\gamma_v$ : ground and volume InSAR coherences

## Interferometric coherence model

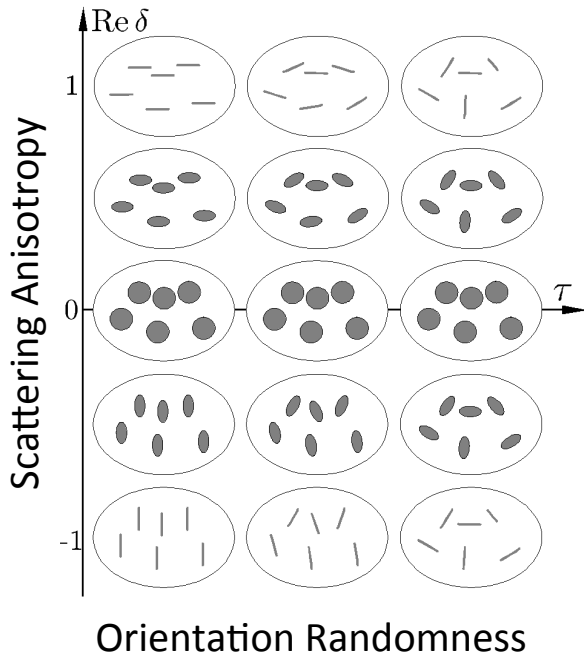
$$\gamma \approx \gamma_{sys} \gamma_{geom} \gamma_z \gamma_{temp}$$

$$\gamma_z = e^{i\phi_0} \int f_0(z) e^{ik_z z} dz, \quad f_0(z) = \frac{e^{\frac{2\sigma}{\cos \theta_0} z}}{\int e^{\frac{2\sigma}{\cos \theta_0} z'} dz'}$$





# Polarimetric Homogeneous Medium Model

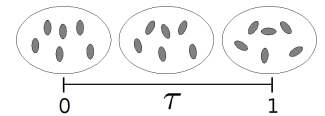
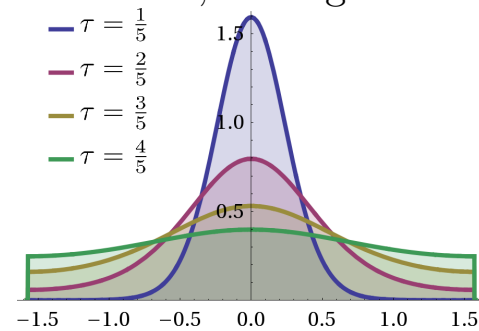


## Orientation Randomness

Circular normal distribution of orientation angles:

$$p(\psi|\tilde{\psi}, \kappa_\psi) = \frac{e^{\kappa_\psi \cos(2(\psi - \tilde{\psi}))}}{\pi I_0(\kappa_\psi)} \quad \tau = \frac{\int p(\psi - \tilde{\psi}) d\psi}{\pi \max p(\psi)} = I_0(\kappa) e^{-\kappa}$$

$\tilde{\psi}$  : main orientation,  $\kappa$  : degree of concentration



## Scattering Anisotropy: Spheroidal Particles

Physical Aspect ratio:

$$r \approx \frac{b}{a} \begin{cases} < 1 & \text{prolate particles} \\ = 1 & \text{spherical particles} \\ > 1 & \text{oblate particles.} \end{cases}$$

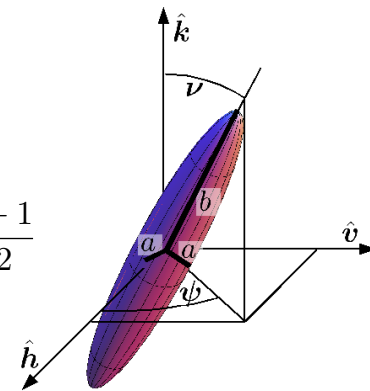
Polarizability Ratio:  $\alpha_r = \frac{\alpha_a}{\alpha_b} = \frac{r + \epsilon_r + 1}{r\epsilon_r + 2}$

Particle Scattering Anisotropy

$$\delta_s(\nu, \alpha_r) = \frac{\alpha_r - 1}{\alpha_r + 1 + 2 \cot^2 \nu}$$

Effective Scattering Anisotropy

$$\delta = \iint \delta_s(\nu, \alpha_r) p(\nu) p(\alpha_r) d\nu d\alpha_r$$



## General formulation:

$$\mathbf{T} = \mathbf{R}_{T(2\tilde{\psi})} \begin{bmatrix} 1 & g_c \delta^* & 0 \\ g_c \delta & \frac{(1+g)}{2} |\delta|^2 & 0 \\ 0 & 0 & \frac{(1-g)}{2} |\delta|^2 \end{bmatrix} \mathbf{R}_{T(2\tilde{\psi})}^T$$

$\mathbf{R}_{T(2\tilde{\psi})}$  : Rotation to main orientation

$$g = \frac{I_2(\kappa)}{I_0(\kappa)}, \quad g_c = \frac{I_1(\kappa)}{I_0(\kappa)}, \quad \tau = I_0(\kappa) e^{-\kappa}$$

\* assumption:  $\delta$  and  $\tau$  uncorrelated



# 2-Layer PolInSAR Vegetation Model

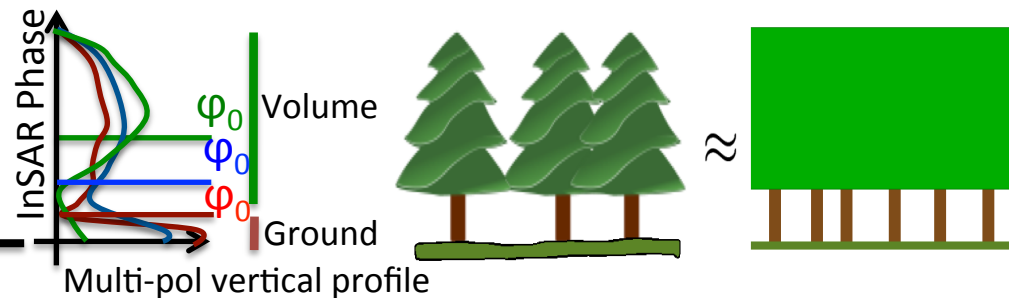
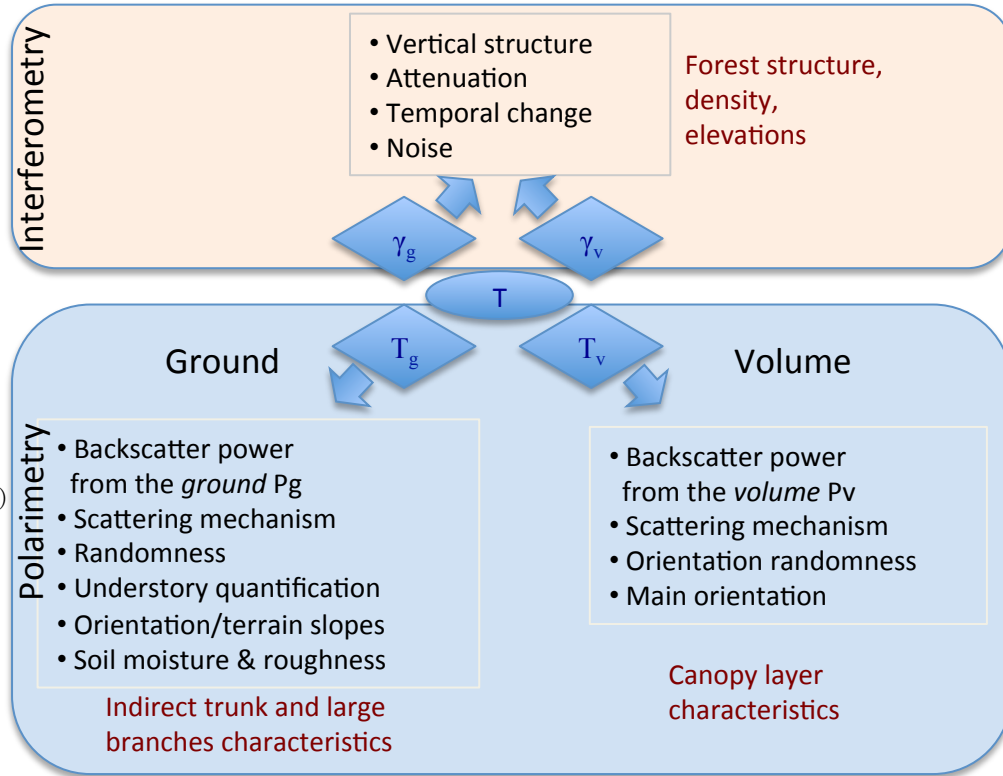
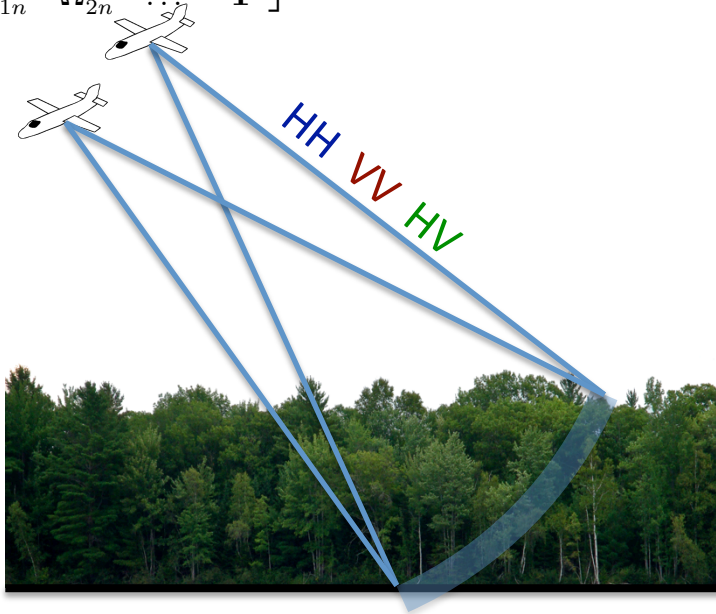
## Single baseline PolInSAR:

$$\mathbf{T}_\delta = \begin{bmatrix} \mathbf{T} & \mathbf{\Omega} \\ \mathbf{\Omega}^\dagger & \mathbf{T} \end{bmatrix} \begin{cases} \mathbf{T} = \mathbf{T}_g + \mathbf{T}_v \\ \mathbf{\Omega} = \gamma_g \mathbf{T}_g + \gamma_v \mathbf{T}_v \end{cases}$$

$$= \mathbf{R}_g \otimes \mathbf{T}_g + \mathbf{R}_v \otimes \mathbf{T}_v \text{ with } \mathbf{R}_{g/v} = \begin{bmatrix} 1 & \gamma_{g/v} \\ \gamma_{g/v}^* & 1 \end{bmatrix}$$

## Multi-baseline PolInSAR:

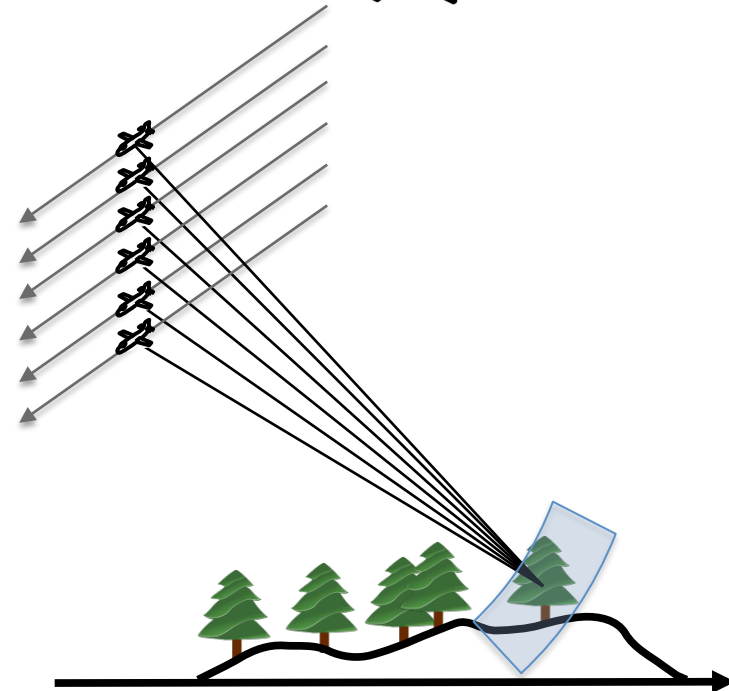
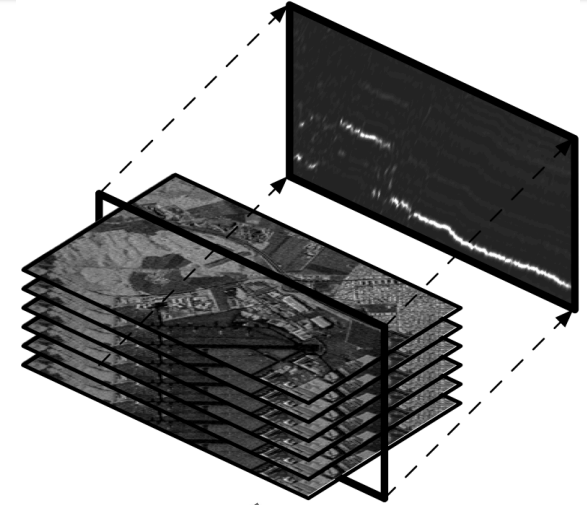
$$\mathbf{T}_{MB} = \begin{bmatrix} \mathbf{T} & \mathbf{\Omega}_{12} & \dots & \mathbf{\Omega}_{1n} \\ \mathbf{\Omega}_{12}^\dagger & \mathbf{T} & \dots & \mathbf{\Omega}_{2n} \\ \vdots & \vdots & \ddots & \vdots \\ \mathbf{\Omega}_{1n}^\dagger & \mathbf{\Omega}_{2n}^\dagger & \dots & \mathbf{T} \end{bmatrix} \rightarrow \begin{cases} \mathbf{T} = \mathbf{T}_g + \mathbf{T}_v \\ \mathbf{\Omega}_{ij} = \gamma_g^{ij} \mathbf{T}_g + \gamma_v^{ij} \mathbf{T}_v \\ \gamma_{g/v}^{ij} \leftarrow \gamma_{g/v}(k_{zij}, \Delta t_{ij}) \end{cases}$$





# SAR Tomography

- SAR Interferometry and SAR Polarimetry:
  - Largely developed at JPL (15-25y ago)
- SAR Tomography:
  - Mainly in Europe (last 10-15y)
  - Initial demonstrations: 10 years ago using airborne (ESAR) and space-borne sensors (ERS-1/2)
  - Potentially high resolution
  - Independent of solar illumination
  - High coverage
- Tomography offers the capability to sense vertically distributed information, e.g., vegetation and ice structure or deformation signals.
  - Extension of 2d SAR imaging to 3d and 4d (space-time).
  - Formation of an additional synthetic aperture in elevation.



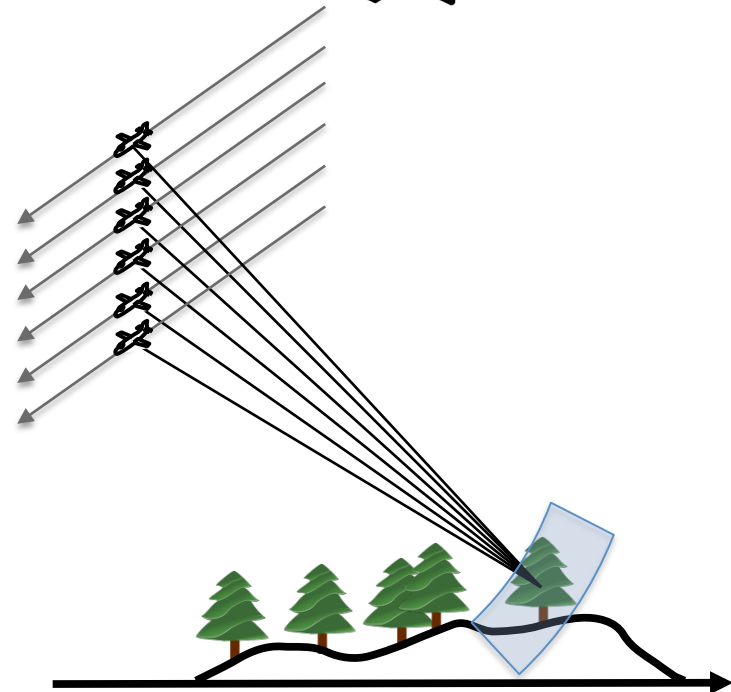
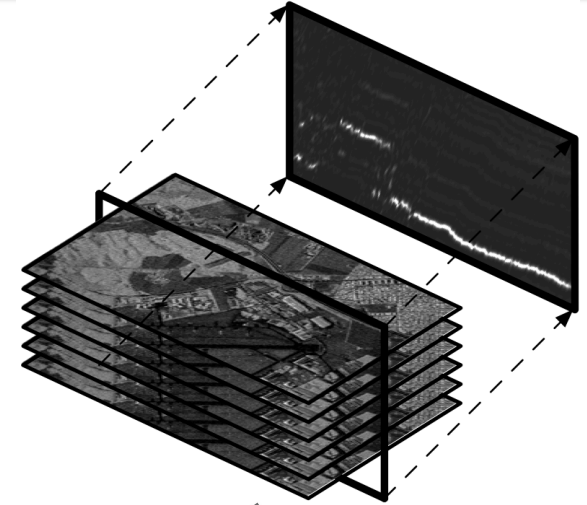
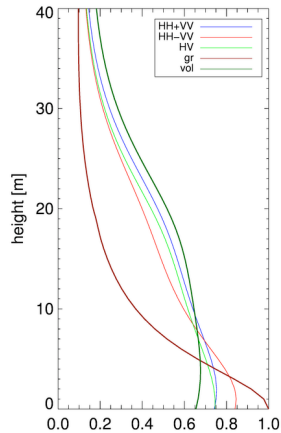
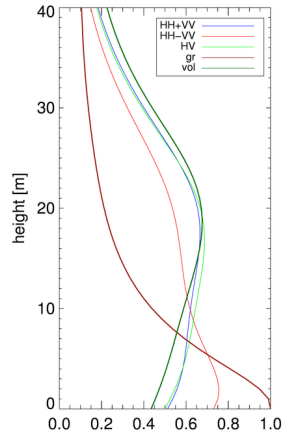
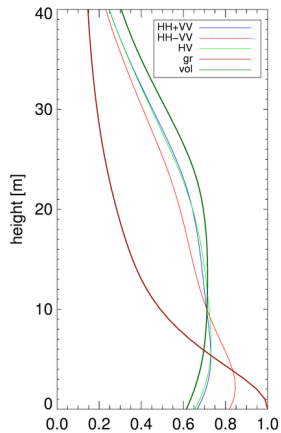
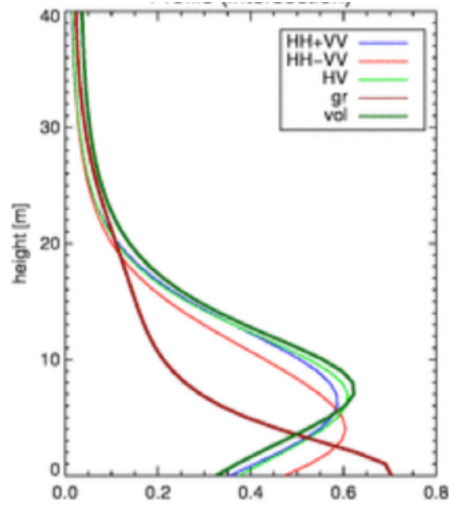




# SAR Tomography

Interpreting Polarimetric SAR Tomography over forests:

- vertical distribution of backscattered energy in dependence of polarization





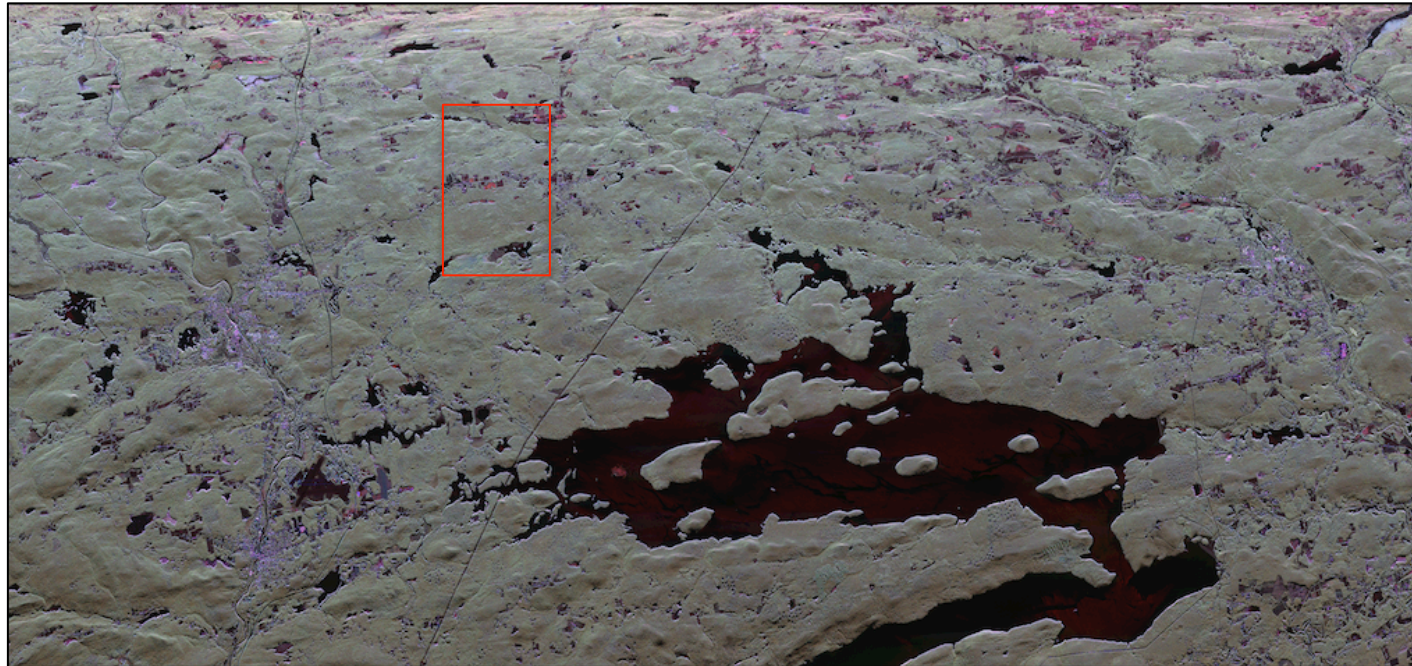
# Experimental Results

## Harvard Forest

JPL's UAVSAR

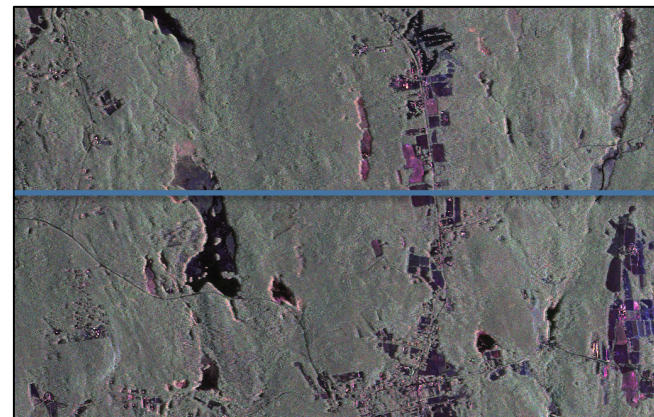
L-band

13 tracks



Spatial baselines: 5m – 125m

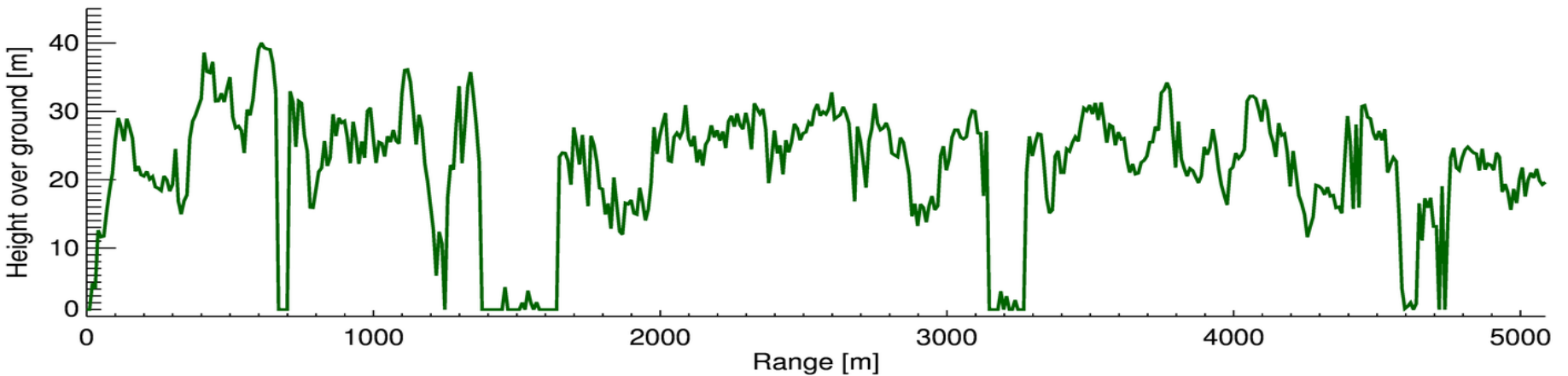
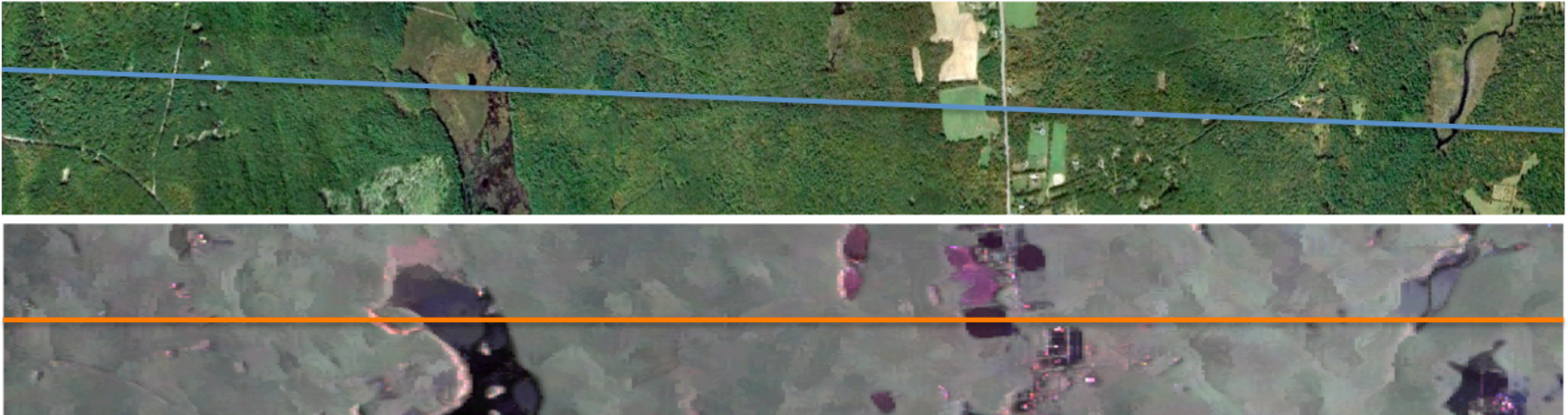
Temporal separation: 30 min – 11 days





# Experimental Results

JPL's UAVSAR sensor – Harvard Forest dataset – L-band

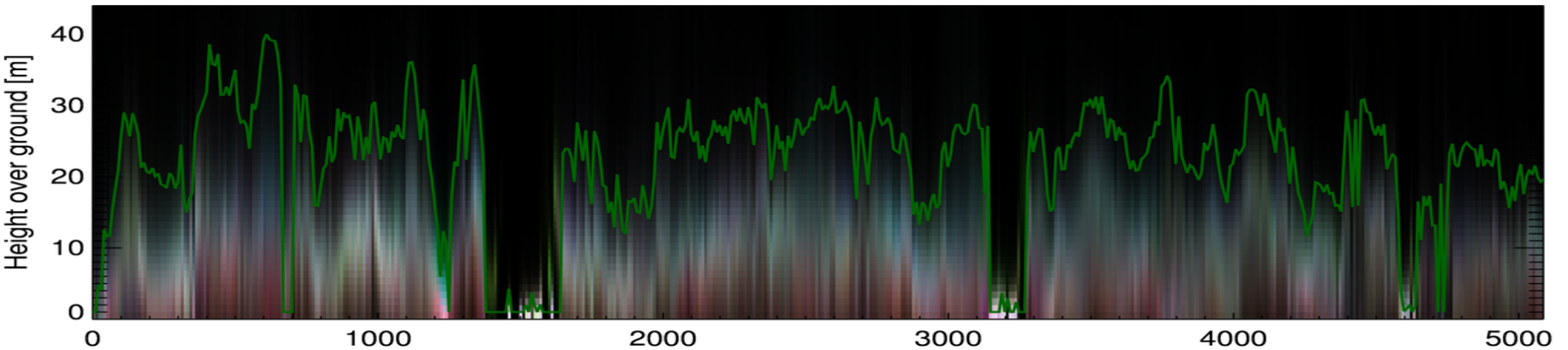


PollnSAR Height Estimate



# Experimental Results

JPL's UAVSAR sensor – Harvard Forest dataset – L-band



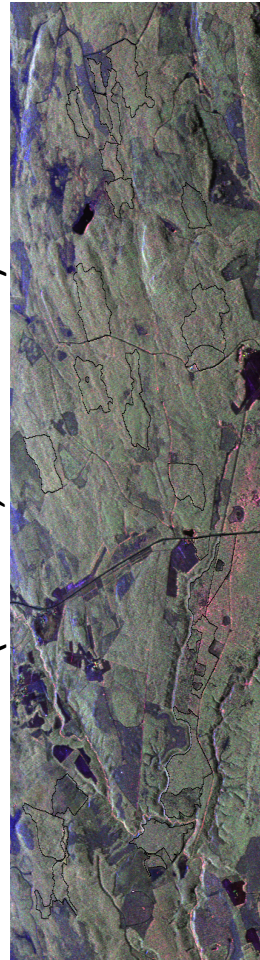
Overlaying PolInSAR Estimate and Pol-Tomogram



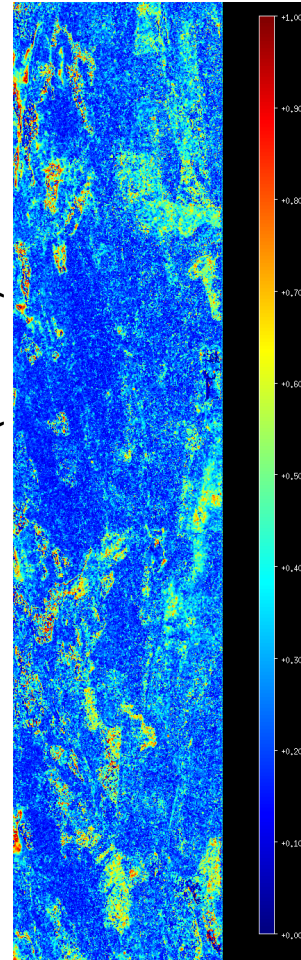
# Experimental Results

- **Krycklan Catchment**
- Northern Sweden Boreal forest
- BioSAR II campaign 2008
- ESA-DLR-FOI-SLU
- DLR's E-SAR sensor
  
- ascending/descending paths
- 6 tracks, respectively
- L- and P-bands
- 2\*27 forest plots

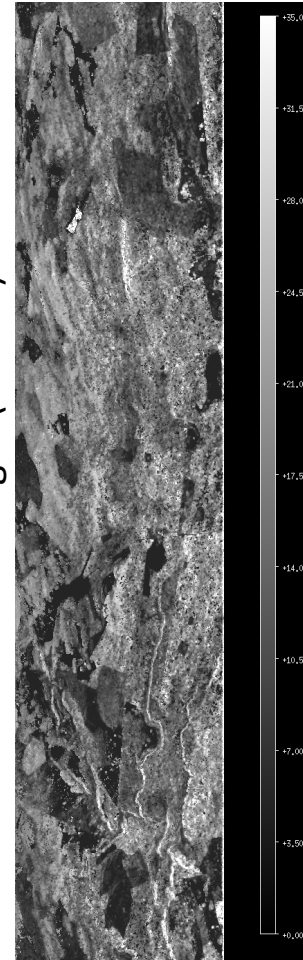
SLC (L-band, Pauli-basis)



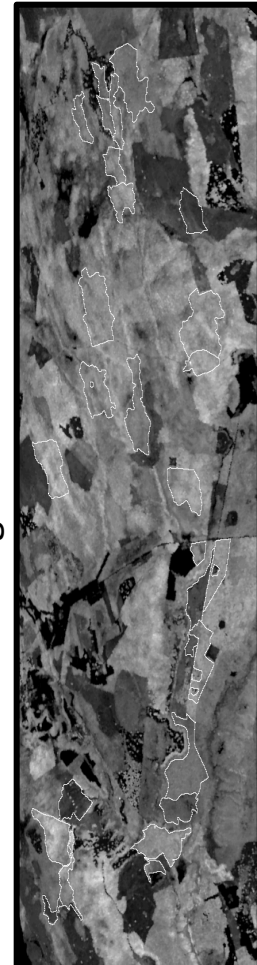
Ground-ratio (L-band)



Estimated height (L-band)

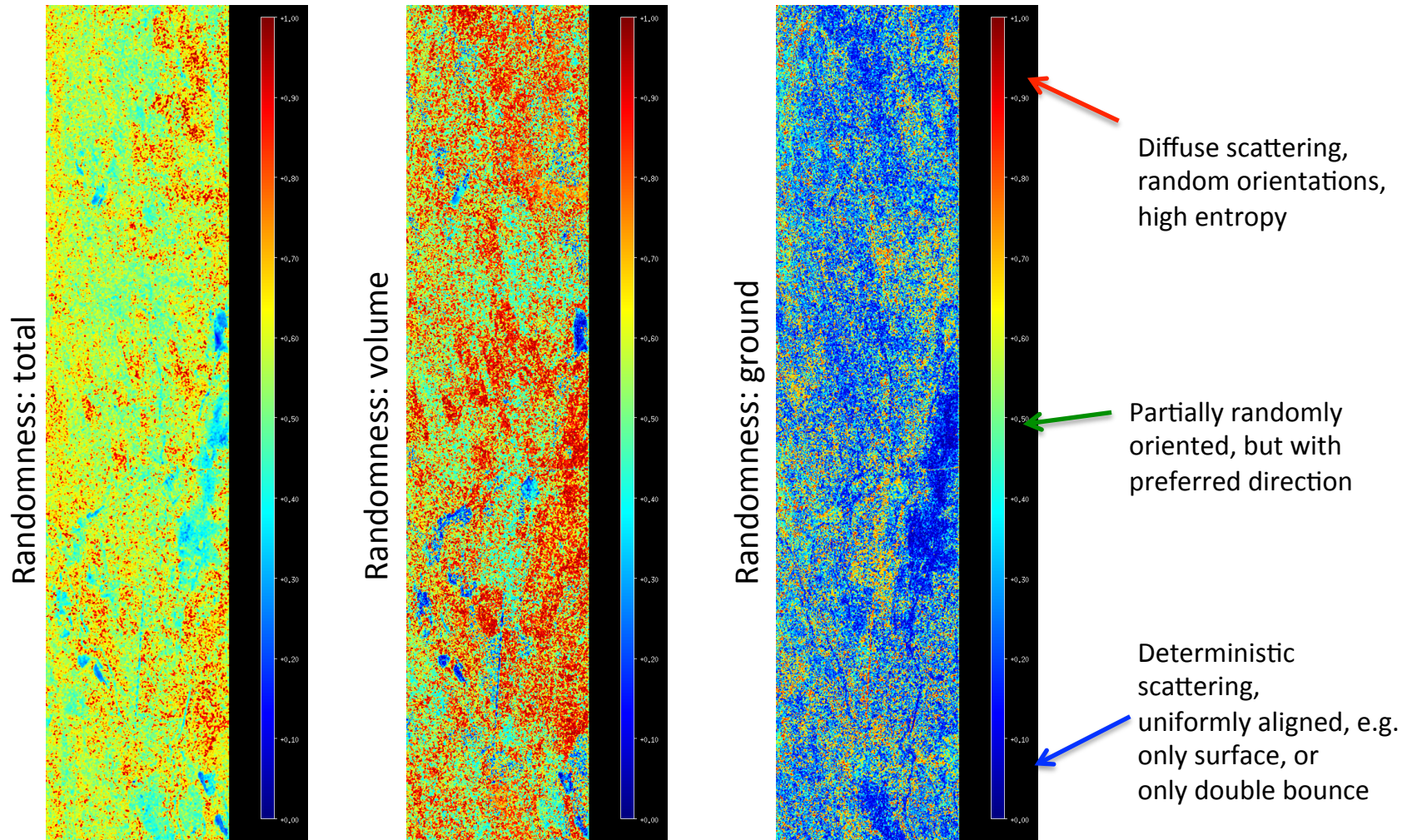


Lidar height - rh100





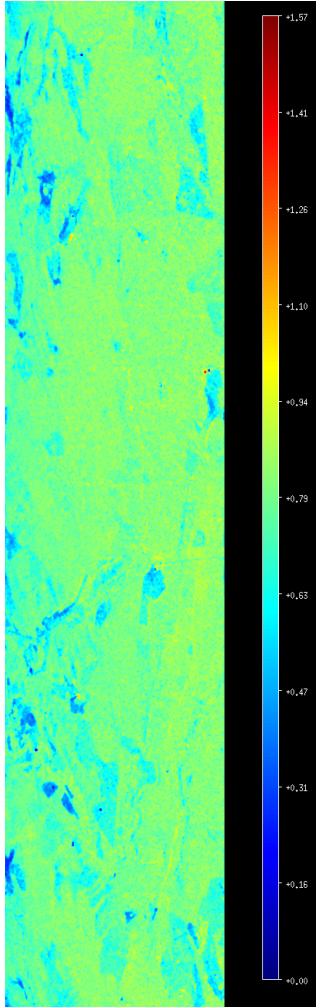
# Experimental Results



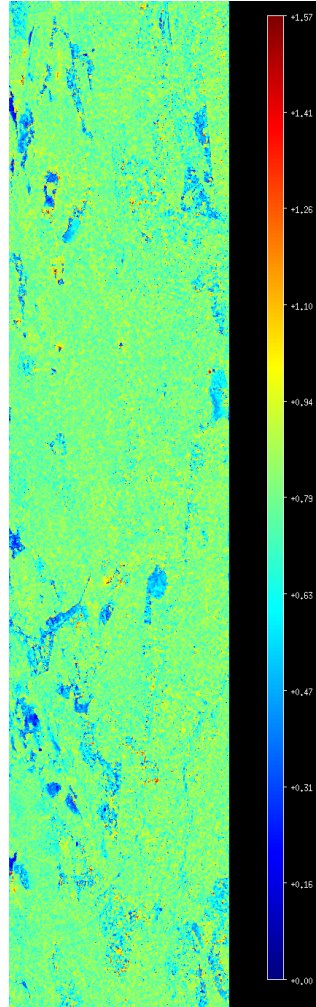


# Experimental Results

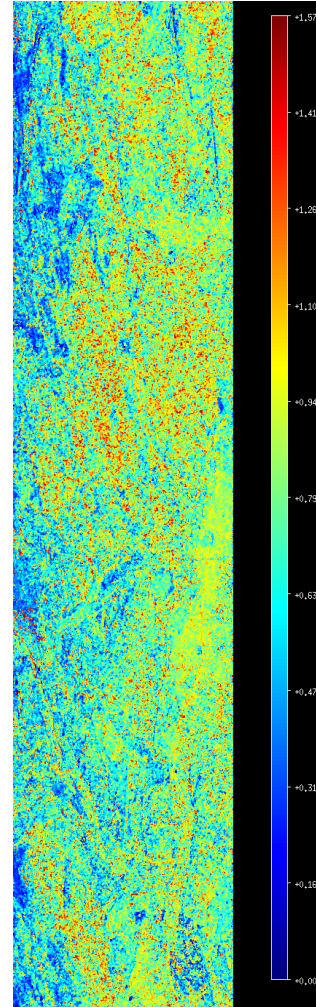
Scattering mechanism type: total



Scattering mechanism type: volume



Scattering mechanism type: ground



Double-bounce  
e.g. trunk-ground,  
branch-branch,  
branch-trunk

Dipole scattering,  
e.g. volume/branch  
particles

Isotropic scattering,  
e.g. surface scattering



# Conclusion

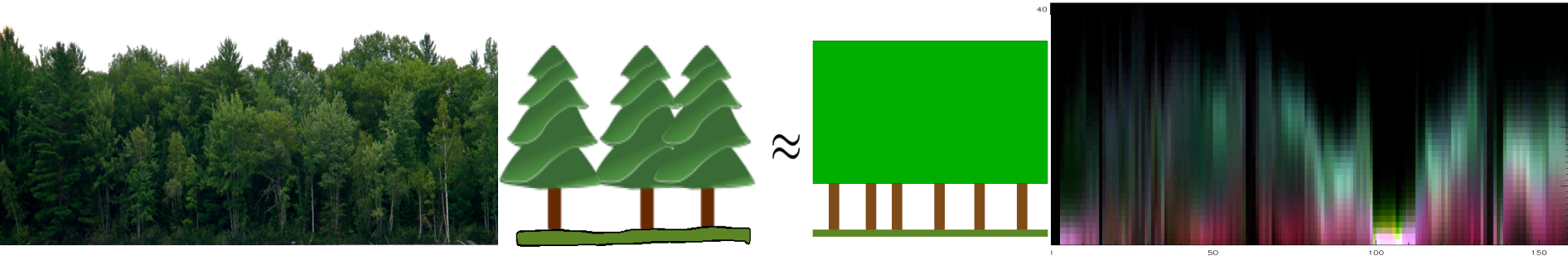
---

- Potential of Polarimetric SAR Interferometry and SAR Tomography for
  - vertical forest structure characterization
  - vegetation and scattering type characterization
- Observations from data:
  - No definitive model which would work for all forests
  - Temporal decorrelation - potentially large error source
  - Strong baseline choice dependence
  - Multiple baselines improve the estimation (\*requires accurate processing & calibration)
  - Performance depends on forest and tree species type
  - L-band: no ground for dense forests, slopes, insufficient double-bounce
- Challenges:
  - Data processing and calibration
  - Long baselines processing for improved height resolution
  - Error analysis



# Forest Structure Characterization using UAVSAR PolInSAR and Tomography

Thank you for your attention!



*UAVSAR Workshop – JPL, Pasadena – 03/27/2013*



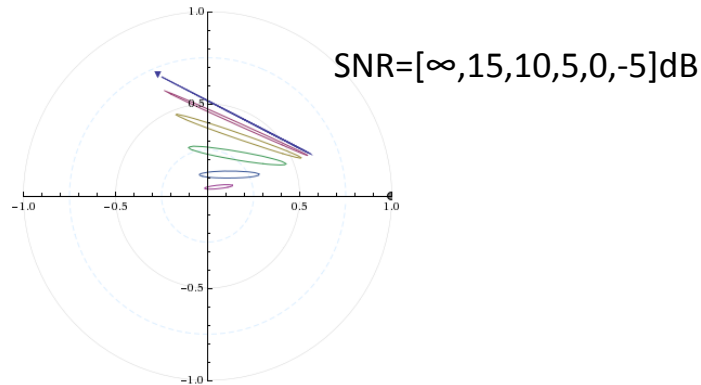
# PolInSAR Coherence Set Distributions

- Example scenario:

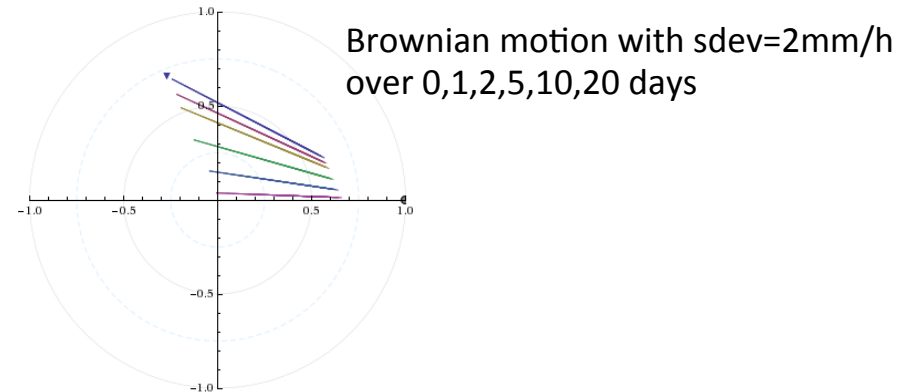
hv=20m, extinction=0.3dB/m, ground phase=0 degree

SNR: [9dB, 15dB], Temporal Brownian motion: 24h with sdev=2mm/h

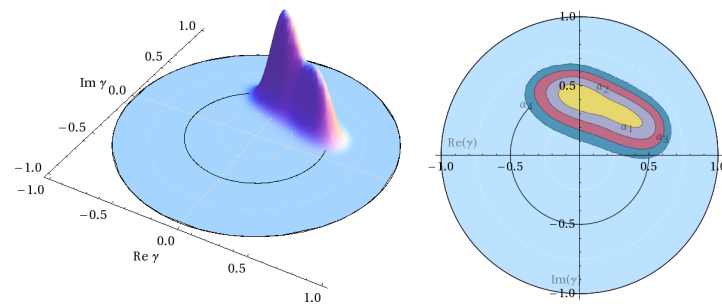
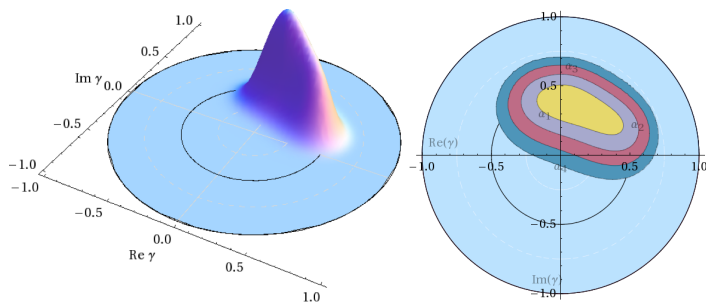
Thermal decorrelation effects:



Temporal decorrelation effects:



A-posteriori cohset PDF's and Confidence regions for 49 and 100 looks:



Confidence levels: 68%, 95.5%, 99.7%, 99.994%



# Non-modeled Variability

- Example PolInSAR height estimation errors due to model simplification. Induced non-modeled coherence magnitude and phase offsets or variabilities, and the resulting height estimation errors, if not compensated.
- Model: simple RVoG
- Example scenario:  
 $h_v=25\text{m}$ , incidence angle=45 degrees,  
 $kz=0.15$ , extinction=0dB.

Error Source	$\Delta \gamma $	$\Delta \arg \gamma$	$\Delta h_v( \gamma )$	$\Delta h_v(\arg \gamma)$
$\gamma_{temp}$ of 0.8	-0.10	$0^\circ$	3.12m	0m
$\sigma_{\gamma_{temp}}$ of 50%	$\pm 0.05$	$0^\circ$	$\pm 1.58\text{m}$	0m
Min( $c_g$ ) of 15%	-0.10	$-20.3^\circ$	2.94m	-4.72m
Canopy 75%	0.19	$13.4^\circ$	-6.25m	3.12m
Extinction 0.2dB/m	0.07	$35.4^\circ$	-2.16m	8.23m
$\sigma_\phi, \sigma_\gamma$ (# looks =25)	$\pm 0.10$	$\pm 13.7^\circ$	$\pm 3.26\text{m}$	$\pm 3.19\text{m}$
$\sigma_\phi, \sigma_\gamma$ (# looks =100)	$\pm 0.05$	$\pm 6.85^\circ$	$\pm 1.61\text{m}$	$\pm 1.60\text{m}$

